Item S1. Supplemental details on the attractiveness score for the redistribution framework

The model calculates location attractiveness using a weighted sum of standardized factors:

$$Attractiveness = W_1(GDP\ Factor) + W_2(Population\ Density\ Factor) + W_3(Climate\ Risk\ Factor)$$

Where:

- Weights (W_1, W_2, W_3) vary by time period
- Climate risk is inversely related to attractiveness (lower risk = higher attractiveness)
- All factors are normalized using z-scores

Weight (W) distributions by time period

Time Period	GDP Weight	Population density Weight	Climate Risk Weight
Near-term (until 2040)	0.329	0.629	0.042
Mid-term (from 2040 - 2070)	0.275	0.658	0.067
Long-term (from 2070 - 2100)	0.217	0.690	0.093

Empirical studies consistently show that economic factors dominate migration decisions relative to environmental factors, though the relative importance varies by context. Studies of agricultural migration [47], West African mobility [48], and flood migration in Bangladesh [49] all demonstrate economic considerations as primary drivers while environmental factors play supporting roles. The model's near-term weights (GDP: 0.329, Climate: 0.042) reflect this empirically observed pattern of economic dominance with climate as a secondary but significant factor.

The model's near-term weights (GDP: 0.329, Climate: 0.042) fall within these empirically observed ranges, with economic factors dominating while climate maintains a statistically significant role.

Academic research also supports adjusting weights over time:

1. **Short-term primacy of economic factors**: Migration research consistently demonstrates that economic considerations typically dominate migration decisions in the near term, with environmental issues serving as generally minor factors compared to economic imperatives, even in highly climate-affected countries [50].
2. **Increasing environmental signal through tipping points**: Several lines of evidence suggest environmental factors may gain importance over time as climate systems approach critical thresholds. Research indicates that exceeding 1.5°C of global warming could trigger multiple climate tipping points—conditions where changes in climate systems become self-perpetuating beyond warming thresholds [51]. These tipping points represent critical thresholds where adaptation capacity may reach limits and environmental changes could accelerate impacts through feedback mechanisms.
3. **Meta-analytical evidence of environmental migration relationships**: Recent meta-analysis of country-level studies provides robust evidence that environmental factors do explain migration patterns, though the magnitude of this relationship strongly depends on particular economic and sociopolitical contexts, with environmental conditions functioning as one of many factors that influence migration rather than operating in isolation [5, 52].

The model incorporates geographic context through spatial weighting of neighboring areas (k-nearest neighbor approach), creating more realistic migration patterns that account for regional proximity effects and spatial spillovers.

Spatial relationships are quantified through a spatial weights matrix (W) that defines neighborhood structure:

1. For each geographic area, the model identifies its K-nearest neighbors (default K=5) based on centroid distances
2. A weights matrix (W) is created where W_{ij} = 1 if area j is a neighbor of area i, and 0 otherwise
3. The weights are row-standardized so that each row sums to 1, ensuring equal influence across areas regardless of neighborhood size

This approach is implemented using K-nearest neighbors (KNN) rather than contiguity-based measures, making it robust for irregular or disconnected geographies and ensuring all areas have exactly K neighbors. The spatial lag operation creates a neighborhood-averaged version of a variable:

$$Spatial\ Lag\ (X_i) = \sum (W_{ij} \times X_j)$$

Where:

- X_i is the value of variable X at location i
- W_{ij} is the spatial weight between locations i and j
- X_j is the value of variable X at location j
- The summation is over all locations j

For attractiveness scores, the spatial lag represents the average attractiveness of neighboring areas, weighted by their spatial proximity.

The final attractiveness score combines direct and spatial components:

$$Final\ Attractiveness\ =\ ((1-S)\ \times\ Direct\ Attractiveness)\ +\ (S\ \times\ Spatial\ Attractiveness)$$

Where:

- S is the spatial weight parameter (default 0.7)
- Direct Attractiveness is based on local attributes (GDP, density, climate risk)
- Spatial Attractiveness is the spatial lag of Direct Attractiveness

This formulation means that an area surrounded by attractive neighbors receives a boost to its own attractiveness, reflecting real-world migration patterns where regions (not just individual locations) tend to attract migrants.

Thereafter, normalized distribution weights are calculated from attractiveness scores:

$$Distribution\ Weight_i = \frac{max(0, Final\ Attractiveness_i)}{\sum\ \ (max(0, Final\ Attractiveness_j)}$$

This ensures all weights are non-negative and sum to 1, creating a probability distribution for migrant allocation.

In the initial raw allocation of inmigrants, and outmigrants are reallocated to their neighboring cells based on their attractiveness distribution:

$$Raw\ Inmigrants_i\ =\ Distribution\ Weight_i \times Total\ Outmigrants$$

Item S2. Supplemental details on migration capacity constraints, excess redistribution, and balance verification within the redistribution framework

Raw allocations are then constrained by location-specific capacity limits:

$$Inmigrants\ (Capped)_i\ =\ min(Raw\ Inmigrants_i, Maximum\ Inmigration_i)$$

Where:

- Maximum In-migration is determined by the growth constraints described below

The capacity-constrained migration approach effectively adapts [53] production-constrained spatial interaction models to apply constraints on the destination side instead. By implementing maximum in-migration thresholds, the model prevents unrealistically high flows to attractive destinations while maintaining the mathematical integrity of the spatial interaction framework. As [54] demonstrate in their analysis of constrained gravity model variants, these "attraction-

constrained" models create a more realistic representation of migration patterns by acknowledging that receiving areas have practical absorption limits.

Time-Dependent Base Growth Rate

$$Base\ Growth\ Rate\ =\ 0.1\ \times\ max(0.5, 1 - (\frac{Y}{75})\ \times 0.5)$$

Where Y is the time period offset (0, 5, 10, etc. years from 2025 baseline).

The time-dependent formulation implements a declining growth pattern consistent with empirical evidence indicating internal migration rates decrease from approximately 7.1% to between 5.0-5.5% over extended periods (Peri & Sasahara, 2019), reflecting the complex non-linear relationships in climate migration dynamics emphasized in recent methodological reviews [55,56]. The declining rate structure aligns with IMF projections indicating migration rates decrease from approximately 7.1% to between 5.0-5.5% over extended periods [57]. This approach incorporates 'demographic amplification' effects where migration patterns adjust dynamically to changing climatic and social conditions [58].

Population Size Adjustment

$$Population\ Size\ Factor\ =\ 1\ -\ (0.5\ \times\ log(Population\ +\ 1)\ /\ max(log(Population\ +\ 1)))$$
$$Adjusted\ Growth\ Rate\ =\ Base\ Growth\ Rate\ \times\ (1\ +\ Population\ Size\ Factor)$$

This logarithmic adjustment captures the well-documented inverse relationship between community size and climate vulnerability observed in migration studies. Rural communities face particular geographic and demographic obstacles in responding to climate change risks due to physical isolation, limited economic diversity, and higher poverty rates, combined with aging populations that increase vulnerability compared to urban areas [59]. Studies confirm that residents of smaller communities are generally more vulnerable to climate disasters due to their diminished emergency response capabilities, lack of emergency medical care, poor hazard warning and emergency management, and poor infrastructure [60, 61]. The logarithmic scaling represents how smaller communities respond more dramatically to climate-induced migration pressures, while larger population centers demonstrate greater resilience through economic and infrastructure advantages.

Cumulative Migration Impact

$$Migration\ Impact\ =\ Cumulative\ Migration\ /\ (Current\ Population\ +\ 1)$$
$$Adjustment\ Factor\ =\ max(0.25, 1\ -\ min(1, Migration\ Impact))$$
$$Final\ Growth\ Rate\ =\ Adjusted\ Growth\ Rate\ \times\ Adjustment\ Factor$$

The cumulative migration impact formula captures the "migration saturation effect" documented in migration systems theory, where destinations exhibit diminishing capacity to absorb additional migrants as the ratio of newcomers to original population increases [62, 63]. This approach aligns with research showing that migration systems can reach limits where network effects

weaken and migration-undermining feedback mechanisms counteract cumulative causation processes [62]. The 0.25 floor ensures migration never completely ceases, reflecting that destinations maintain some baseline capacity for migration flows even under high-saturation conditions, consistent with empirical observations that migration networks retain some functionality even when their facilitating effects diminish [64].

Population Threshold Graduation

Different growth rules apply based on population level:

- **Normal areas** (100+ people): Standard growth limits apply
- **Low population areas** (1-100 people): Slightly higher percentage growth allowed
- **Zero/near-zero population areas**: Extremely restrictive conditions (must be highly attractive AND near populated regions)

The population threshold graduation approach reflects established migration patterns showing that settlement change typically follows hierarchical systems, with step migration occurring where "the main destination of permanent net-out-migration is to nearby towns" rather than direct movement to large metropolitan areas [65]. This approach aligns with research demonstrating that human settlements are predominantly "distributed in urban agglomerations and coastal areas" with growth concentrated in established population centers [66], and that migration patterns show "strong rural and urban links" and bidirectional flows between settlement types, suggesting that population growth occurs through established networks rather than creating entirely new settlements [65]. The restrictive conditions for zero-population areas reflect empirical findings that migration streams follow existing social networks and proximity to established communities, with settlement patterns being path-dependent on existing population distributions.

Lifetime Growth Multiplier

$$Maximum\ Growth\ =\ Base\ Year\ Population\ \times\ Lifetime\ Multiplier$$

Where Lifetime Multiplier increases gradually from 5× in early periods to 15× in later periods.

The Lifetime Growth Multiplier approach operationalizes research showing that urban carrying capacity "determines the scale and development direction" of destinations and evolves as communities develop infrastructure over time [67]. The gradual increase from 5× to 15× reflects findings that destinations can enhance their absorptive capacity through "elaborated integration of urban and transportation planning, including aspects of land use and building floor area regulation" [68], while the temporal constraint aligns with urban planning research demonstrating that "practical approaches which incorporate the concept of carrying capacity into managing urban development" recognize that infrastructure and settlement capacity develop progressively rather than remaining static [69].

Excess Migrant Redistribution

If capacity constraints create excess migrants (migrants that cannot be accommodated in their most attractive destinations), they are redistributed:

$$Remaining\ Capacity_i = Maximum\ Inmigration_i - Inmigrants\ (Capped)_i$$

$$Excess\ Distribution\ Weight_i = \frac{Remaining\ Capacity_i}{\sum \quad Remaining\ Capacity_j}$$

$$Excess\ Inmigrants_i = Excess\ Distribution\ Weight_i \times Total\ Excess\ Migrants$$

$$Adjusted\ Inmigrants_i = Inmigrants\ (Capped)_i\ + Excess\ Inmigrants_i$$

This iterative rebalancing procedure follows principles similar to iterative proportional fitting methods used in transportation modeling [70, 71], ensuring all migrants are allocated while respecting locational capacity constraints.

The final stage ensures perfect balance between total outmigrants and in-migrants while preserving the underlying attractiveness gradient, addressing flow conservation requirements fundamental to spatial interaction models where migration balance constraints are essential for demographic consistency [53, 72, 73].

Balance Verification

The model checks if total in-migrants equals total outmigrants:

$$Difference\ = \sum \quad (Inmigrants_i)\ - \sum \quad (Outmigrants_i)$$

If the difference is zero, no adjustment is needed.

Attractiveness-Preserving Adjustment

If the difference is greater than zero, adjustment is needed, and the model makes minimal changes that respect attractiveness patterns:

If Inmigrants Exceed Outmigrants:

The model creates a composite unattractiveness score that combines inverse attractiveness with current inmigrant allocation:

$$Unattractiveness\ Score_i\ = 0.7 \times Rank(\frac{1}{Final\ Attractiveness_i})\ + 0.3 \times Rank(Inmigrants_i)$$

Migrants are removed first from areas with the highest composite score (least attractive areas with substantial inmigrants), preserving the principle that the most attractive destinations should retain their migrants [6, 74].

If Inmigrants Fall Short of Outmigrants:

Migrants are added to locations in strict attractiveness order:

1. First to attractive areas with remaining capacity: $Inmigrants_i < Maximum\ Inmigration_i$
2. If insufficient capacity exists, to the most attractive areas regardless of capacity

This approach preserves the core principle that climate migrants move to the most suitable destinations, which is supported by empirical studies of amenity migration [24, 75]

After balancing, net migration and cumulative migration values are updated:

$$Net\ Migration_i = Inmigrants_i - Outmigrants_i$$

$$Cumulative\ Migration_i = Cumulative\ Migration_i + Net\ Migration_i$$

These final balanced values are used to "climate-correct" the SSP population projections, providing a more realistic spatial distribution of population under climate change scenarios [6].

Item S3. Cross-Scenario Comparison

Figure S1 displays projected net climate-driven migration patterns across three Shared Socioeconomic Pathways (SSPs) for 2100. The maps illustrate how climate-induced displacement creates redistribution flows toward economically resilient regions. Areas experiencing negative net migration represent climate-vulnerable zones where environmental risks drive population outflows, concentrated across sub-Saharan Africa, parts of South and Southeast Asia, small island states, and portions of Latin America.

The positive net migration areas represent economically robust destinations with the infrastructure, labor markets, and institutional capacity to absorb climate migrants. The escalating displacement magnitude across scenarios reflects how different development pathways affect both climate pressures and economic disparities. SSP5's extreme range (-327,931 to 156,206) suggests that high-inequality development creates both severe climate displacement and concentrated economic opportunities in select regions.

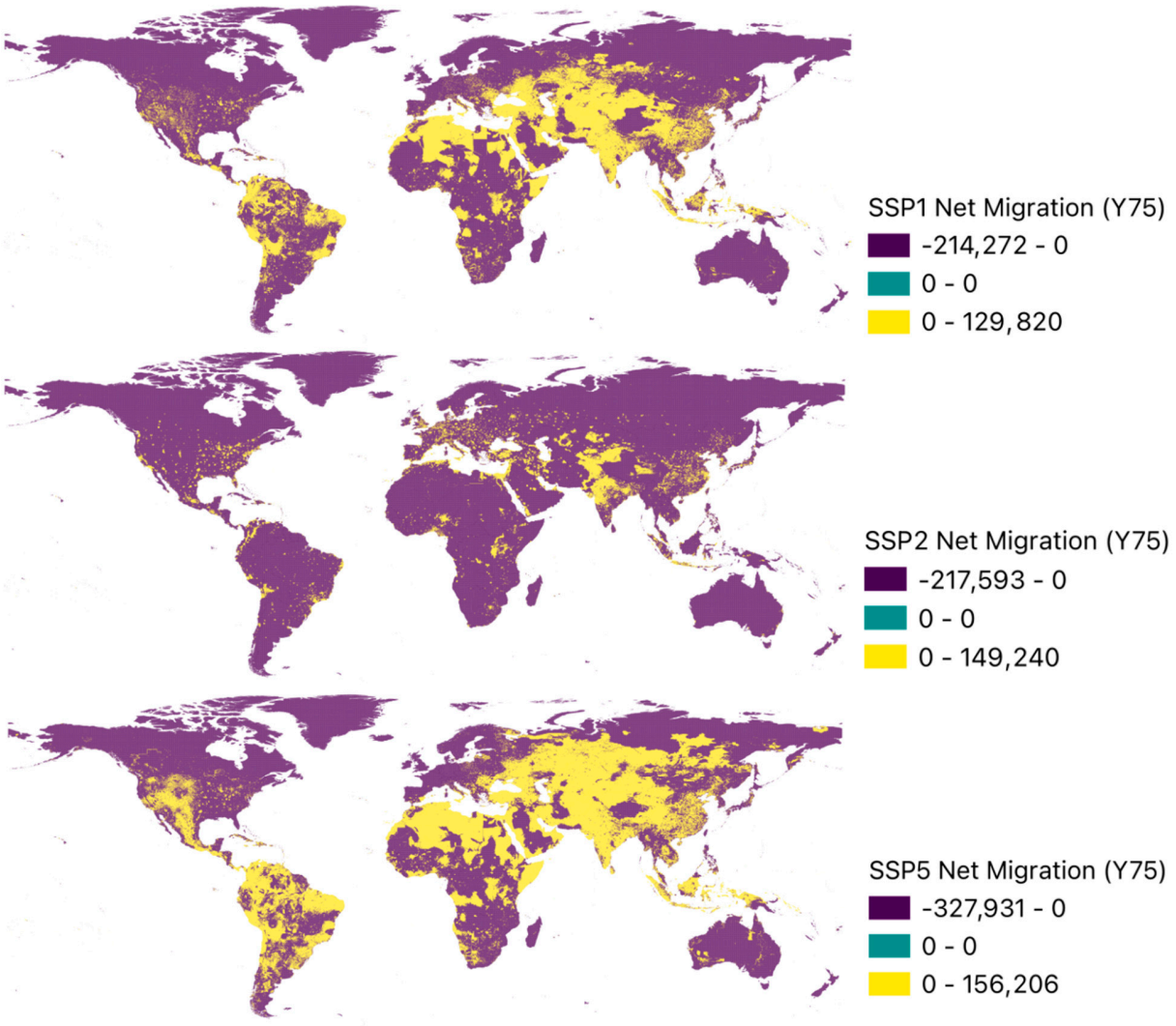


Figure S1. Global patterns of net migration in year 75 accounting for climate migration and migrant redistribution across SSP1, SSP2, and SSP5.

50. de Haas, H. (2010). Migration and Development: A Theoretical Perspective. International Migration Review, 44(1), 227–264. https://doi.org/10.1111/j.1747-7379.2009.00804.x
51. McKay, D. I. A., Staal, A., Abrams, J. F., Winkelmann, R., Sakschewski, B., Loriani, S., Fetzer, I., Cornell, S. E., Rockström, J., & Lenton, T. M. (2022). Exceeding 1.5°C global warming could trigger multiple climate tipping points. Science, 377(6611), eabn7950. https://doi.org/10.1126/science.abn7950
52. Ou-Salah, H., Boas, I., & Warner, J. (2022). The role of environmental factors and other migration drivers from the perspective of Moroccan and Congolese migrants in Belgium. Comparative Migration Studies, 10, 307. https://doi.org/10.1186/s40878-022-00307-y
53. Wilson, A. G. (1971). A Family of Spatial Interaction Models, and Associated Developments. Environment and Planning A: Economy and Space, 3(1), 1–32. https://doi.org/10.1068/a030001
54. Griffith, D. A., & Fischer, M. M. (2013). Constrained variants of the gravity model and spatial dependence: Model specification and estimation issues. Journal of Geographical Systems, 15(3), 291–317. https://doi.org/10.1007/s10109-013-0182-7

55. Peri, G., & Sasahara, A. (2019). The impact of global warming on rural-urban migrations: Evidence from global big data. NBER Working Paper No. 25728.
56. Beyer RM, Schewe J and Abel GJ (2023) Modeling climate migration: dead ends and new avenues. Front. Clim. 5:1212649. doi: 10.3389/fclim.2023.1212649
57. Cattaneo, C., Massetti, E., Dasgupta, S., & Farinosi, F. (2024). Climate Variability and Worldwide Migration: Empirical Evidence and Projections. IMF Working Papers, 2024(058), A001. https://doi.org/10.5089/9798400270772.001.A001
58. Hauer, M. E., Jacobs, S. A., & Kulp, S. A. (2024). Climate migration amplifies demographic change and population aging. Proceedings of the National Academy of Sciences, 121(3), e2206192119. https://doi.org/10.1073/pnas.2206192119
59. National Climate Assessment. (2014). Rural Communities. U.S. Global Change Research Program. https://nca2014.globalchange.gov/highlights/regions/rural-communities. Accessed 07/30/25.
60. Birkmann, J., Welle, T., Solecki, W., Lwasa, S., & Garschagen, M. (2016). Boost resilience of small and mid-sized cities. Nature, 537(7622), 605-608.
61. Cross, J. A. (2001). Megacities and small towns: Different perspectives on hazard vulnerability. Environmental Hazards, 3(2), 63-80.
62. de Haas, H. (2010). The internal dynamics of migration processes: A theoretical inquiry. Journal of Ethnic and Migration Studies, 36(10), 1587-1617. https://doi.org/10.1080/1369183X.2010.489361
63. Fussell, E., & Massey, D. S. (2004). The limits to cumulative causation: International migration from Mexican urban areas. Demography, 41(1), 151-171.
64. Light, I., Bhachu, P., & Karageorgis, S. (1993). Migration networks and immigrant entrepreneurship. In I. Light & P. Bhachu (Eds.), Immigration and entrepreneurship: Culture, capital, and ethnic networks (pp. 25-49). Transaction Publishers.
65. Collinson, M. A., Tollman, S. M., Kahn, K., Clark, S. J., & Garenne, M. (2007). Migration, settlement change and health in post-apartheid South Africa: Triangulating health and demographic surveillance with national census data. Population Health Metrics, 5, 9.
66. Liu, S., Zhang, P., Wang, Z., Li, Z., Wang, X., & Yang, Y. (2021). Changes in the geographical distributions of global human settlements. Journal of Resources and Ecology, 12(6), 776-788.
67. Liu, Z., Wang, S., & Fang, C. (2022). Urban comprehensive carrying capacity and development order: A "pressure-capacity-potential" logical framework. Frontiers in Environmental Science, 10, 935498.
68. Chen, Y. J., Yeh, K., & Lo, S. C. (2024). Away from over-populated development: Estimating urban carrying capacity with an integrated perspective of transportation and urban planning. Transportation Research Part A: Policy and Practice, 190, 104246.
69. Oh, K., Jeong, Y., Lee, D., Lee, W., & Choi, J. (2005). Determining development density using the Urban Carrying Capacity Assessment System. Landscape and Urban Planning, 73(1), 1-15.
70. Furness, K. P. (1965). Time function iteration. Traffic Engineering and Control, 7(7), 458-460.
71. Evans, A. W. (1970). Some properties of trip distribution methods. Transportation Research, 4(1), 19-36.
72. Bell, M., & Muhidin, S. (2009). Cross-national comparisons of internal migration (Human Development Research Paper 2009/30). United Nations Development Programme.
73. Willekens, F. (2016). Migration flows: Measurement, analysis and modeling. In M. J. White (Ed.), International handbook of migration and population distribution (pp. 225-241). Springer. https://doi.org/10.1007/978-94-017-7282-2_11
74. McLeman, R. (2018). Thresholds in climate migration. Population and Environment, 39, 319–338.
75. Findlay, A. M. (2011). Migrant destinations in an era of environmental change. Migration and Global Environmental Change – Review of Drivers of Migration, 21, S50–S58. https://doi.org/10.1016/j.gloenvcha.2011.09.004